Available online at www.sciencedirect.com
ScienceDirect
Polymer 49 (2008) 800–808
polymer
www.elsevier.com/locate/polymer

Effect of chemisorption on the interfacial bonding characteristics of carbon nanotube–polymer composites

Qingbin Zheng, Qingzhong Xue*, Keyou Yan, Xili Gao, Qun Li, Lanzhong Hao

Department of Material Physics, College of Physics Science and Technology, China University of Petroleum, 271, Beier Road, Dongying, Shandong 257061, People's Republic of China

Received 18 July 2007; received in revised form 13 December 2007; accepted 16 December 2007
Available online 23 December 2007

Abstract

The influence of chemical functionalization on the interfacial bonding characteristics of single-walled nanotubes (SWNTs) reinforced polymer composites was investigated using molecular mechanics and molecular dynamics simulations. The simulations show that functionalization of nanotubes at low densities of functionalized carbon atoms drastically increases their interfacial bonding and shear stress between the nanotubes and the polymer matrix, where chemisorption to as little as 5.0% of the nanotube carbon atoms increases the shear stress by about 1000%. This indicates that increasing the load transfer between SWNTs and a polymer matrix in a composite via chemisorption may be an effective way and chemical attachment of nanotubes during processing may be in part responsible for the enhanced stress transfer observed in some systems of the nanotube–polymer composites. Furthermore, this suggests the possibility to use functionalized nanotubes to effectively reinforce other kinds of polymer-based materials as well.

Keywords: Carbon nanotube polymer composites; Simulation; Chemical functionalization

1. Introduction

Since the discovery of carbon nanotubes (CNTs) by Iijima in 1991 [1], CNTs have attracted great research interest due to their unique properties such as high electrical and thermal conductivity, excellent stiffness against bending, and high tensile strength [2]. Using CNTs as nanofibers to enhance the mechanical [3–10], electrical [11–14], thermal [15–17], and optical [18] properties of composite materials has been pursued extensively both in experimental and theoretical studies. Recently, experiments have shown remarkable enhancements in elastic modulus and strength of polymer composites with an addition of small amounts of CNTs [19–22]. Despite these first successes, some critical issues, such as the uniform dispersion and alignment of the nanotubes within the polymer matrix, must be overcome before the full potential of CNTs can be realized. Another most significant challenging issue is the interfacial bonding between the nanotubes and the polymer matrix, which determines the efficiency of load transfer from the polymer matrix to the nanotubes [23]. It is well established, from the research on microfiber-reinforced composites over the past few decades, that the structure and properties of the fiber–matrix interface play a major role in determining mechanical performance and structural integrity of composite materials. In order to take advantage of the very high Young's modulus and strength of CNTs, an efficient load transfer from the polymer matrix to the nanotubes is required. Due to high aspect ratio of the CNTs, large areas are available for load transfer in CNT–polymer composites, which are unlike conventional fiber-reinforced polymer composites. However, due to their unique electrical and structural properties, CNTs tend not to bond strongly with their host matrix. As a result, the potential increases and improvements in the mechanical properties of a nanotube-reinforced composite are limited by the degree of interfacial stress transfer that can be achieved. One possible way to improve the interfacial bonding between

* Corresponding author. Tel.: +86 0546 839 2836; fax: +86 0546 839 2123.
E-mail address: xueqingzhong@tsinghua.org.cn (Q. Xue).

0032-3861/$ - see front matter © 2007 Elsevier Ltd. All rights reserved.
doi:10.1016/j.polymer.2007.12.018

CNTs and a supported matrix is by chemically functionalizing the CNTs into the matrix, such as chemical attachment or cross-linking of CNTs with polymeric matrix. However, due to difficulties in devising experiments to study the CNT–polymer interface, molecular mechanics (MM) and molecular dynamics (MD) simulations have become increasingly popular in the investigations of reinforcement mechanisms in CNT–polymer composite systems [24]. Many groups have investigated the interfaces in CNT-reinforced polymer composites using MM and MD simulations.

The MM study of interfacial binding of CNT–polymer composites was first conducted by Lordi and Yao [25]. Force-field-based MM calculations were performed to determine binding energies and sliding frictional stresses to understand the factors governing interfacial adhesion. The results showed that the binding energies and frictional forces played only a minor role in determining the strength of the interface, but the helical polymer conformations were essential. It was suggested that the strength of the interface may be mostly due to molecular-level entanglement of the two phases and forced long-range ordering of the polymer. Liao and Li [26] have studied the interfacial characteristics of a CNT-reinforced polystyrene (PS) composite system through MM simulations and elasticity calculations. They found that the fiber–matrix adhesion comes from electrostatic interaction, van der Waals interaction, mismatch in the coefficients of thermal expansion and radial deformation induced by atomic interactions. Frankland et al. [27] have investigated the influence of chemical cross-links between a single-walled nanotube (SWNT) and a polymer matrix on the matrix-nanotube shear strength using MD simulations. The results suggested that load transfer and modulus of nanotube–polymer composites could be effectively increased by deliberately adding chemical cross-linking and inadvertent chemical bonding between nanotubes and polymer matrices during processing that may be in part responsible for the enhanced stress transfer observed in some systems of this type. Wong et al. [28] have studied local fracture morphologies of CNT–PS rod and CNT–epoxy film composites. Transmission and scanning electron microscopy examinations showed that these polymers adhered well to CNT at the nanometer scale. Some of the important interfacial characteristics that critically control the performance of a composite material were quantified through MM simulations and elasticity calculations. Multi-walled CNT morphology-related mechanical interlocking at nanometer scale, thermal residual stresses, as well as relatively cavity free surface for polymer adsorption were also believed to be the contributing factors. Gou et al. [23] investigated the interfacial bonding of SWNT-reinforced epoxy composites using a combination of computational and experimental methods. The interfacial shear strength between the nanotube and the cured epoxy resin was calculated to be up to 75 MPa, indicating that there could be an effective stress transfer from the epoxy resin to the nanotube. The following experimental results provided evidence of stress transfer in agreement with the simulation results. Yang et al. [29] have studied the interaction between polymers and CNTs using force-field-based MD simulation. They found that the specific monomer structure plays a very important role in determining the strength of interaction between nanotubes and polymers. The polymers with a backbone containing aromatic rings were promising candidates for the non-covalent binding of CNTs into composite structures, which could be used as building blocks in amphiphilic copolymers to promote increased interfacial binding between the CNT and the polymeric matrix. Wei [30] has studied temperature dependent adhesion behavior and reinforcement in CNT–polymer composite. They found that the interfacial shear stress through van der Waals interactions increases linearly with applied tensile strains along the nanotube axis direction and a lower bound value for the shear strength is found to be $\sim$46 MPa at low temperatures. Direct stress–strain calculations showed significant reinforcements in the composite in a wide temperature range, with $\sim$200% increase in the Young's modulus when adding 6.5% volume ratio of short CNTs.

While chemically cross-linking or molecular entanglement method to strengthen the interface has been conducted [25,27], studies involving the influence of chemical attachment on interfacial properties of CNTs have not been reported. This report was about finding a viable way to get SWNT to go into the polymer matrix to act as reinforcement. The difficulties involved in doing this arise mostly from the fact that CNTs cannot interact well with other materials. The method pursued here for making the SWNTs capable of effectively interacting with the polymer was based on the covalent attachment of functional groups to the surface of SWNTs. By taking advantage of these functional groups, which could act as an effective interfacial bridge between the SWNTs and the polymeric matrix, an effective load transfer could be achieved between the SWNTs and the polymer matrix. In this study, the influence of chemical functionalization on the interfacial bonding between the SWNTs and polymer was investigated using MM and MD simulations.

2. Experimental

2.1. Computational method

In the CNT–polymer composite systems, the dimension of the nanotube is about the same size as a polymer chain and hence the discrete nature of the atomic interactions between the nanotubes and surrounding polymer matrix should be taken into account. In other words, the nature of the load transfer should be understood using physical based analysis, where MM and MD simulations will be the most important tools [31]. In this work, MM and MD simulations were conducted to explore the interfacial bonding characteristics between the SWNTs and the polymer, through which we could get useful information for the development of nanotube-based polymeric composites. Here, MM and MD simulations were carried out using a commercial software package called Materials Studio developed by Accelrys Inc. The condensed phase optimization molecular potentials for atomistic simulation studies (COMPASS) module in the Materials Studio software was used to conduct force-field computations. The COMPASS is a parameterized, tested and validated first ab initio force field [32,33],

which enables an accurate prediction of various gas-phase and condensed phase properties of most of the common organic and inorganic materials [34–36].

2.2. Force field

The application of quantum mechanical techniques can accurately simulate a system of interacting particles, but such techniques often cost too much time and are usually feasible only in systems containing up to few hundreds of interacting particles. As we know, the main goal of simulations of the systems containing a large number of particles is generally to obtain the systems' bulk properties which are primarily controlled by the location of atomic nuclei, so the knowledge of the electronic structure, provided by the quantum mechanic techniques, is not critical. Thus, we could have a good insight into the behavior of a system if a reasonable, physically-based approximation of the potential (force field) can be obtained, which can be used to generate a set of system configurations which are statistically consistent with a fully quantum mechanical description. As stated above, a crucial point in the atomistic simulations of multi-particle systems is the choice of the force fields, a brief overview of which is given in this section.

In general, the total potential energy of a molecular system includes the following terms [37]:

$$E_{\text{total}} = E_{\text{valence}} + E_{\text{cross-term}} + E_{\text{non-bond}} \tag{1}$$

$$E_{\text{valence}} = E_{\text{bond}} + E_{\text{angle}} + E_{\text{torsion}} + E_{\text{oop}} + E_{\text{UB}} \tag{2}$$

$$\begin{aligned} E_{\text{cross-term}} = {} & E_{\text{bond-bond}} + E_{\text{angle-angle}} + E_{\text{bond-angle}} \\ & + E_{\text{end-bond-torsion}} + E_{\text{middle-bond-torsion}} \\ & + E_{\text{angle-torsion}} + E_{\text{angle-angle-torsion}} \end{aligned} \tag{3}$$

$$E_{\text{non-bond}} = E_{\text{vdW}} + E_{\text{Coulomb}} + E_{\text{H-bond}} \tag{4}$$

The valence energy, E_{valence}, generally includes a bond stretching term, E_{bond}, a two-bond angle term, E_{angle}, a dihedral bond-torsion term, E_{torsion}, an inversion (or an out-of-plane interaction) term, E_{oop}, and a Urey–Bradlay term (involves interactions between two atoms bonded to a common atom), E_{UB}. The cross-term interacting energy, $E_{\text{cross-term}}$, generally includes: stretch–stretch interactions between two adjacent bonds, $E_{\text{bond-bond}}$, bend–bend interactions between two valence angles associated with a common vertex atom, $E_{\text{angle-angle}}$, stretch–bend interactions between a two-bond angle and one of its bonds, $E_{\text{bond-angle}}$, stretch–torsion interactions between a dihedral angle and one of its end bonds, $E_{\text{end-bond-torsion}}$, stretch–torsion interactions between a dihedral angle and its middle bond, $E_{\text{middle-bond-torsion}}$, bend–torsion interactions between a dihedral angle and one of its valence angles, $E_{\text{angle-torsion}}$, and bend–bend–torsion interactions between a dihedral angle and its two valence angles, $E_{\text{angle-angle-torsion}}$. The non-bonded interaction term, $E_{\text{non-bonded}}$, accounts for the interactions between non-bonded atoms and includes the van der Waals energy, E_{vdW}, the Coulomb electrostatic energy, E_{Coulomb}, and the hydrogen bond energy, $E_{\text{H-bond}}$.

The COMPASS force field uses different expressions for various components of the potential energy as follows [34,35]:

$$\begin{aligned} E_{\text{valence}} = {} & \sum_b \left[K_2(b-b_0)^2 + K_3(b-b_0)^3 + K_4(b-b_0)^4\right] \\ & + \sum_\theta \left[H_2(\theta-\theta_0)^2 + H_3(\theta-\theta_0)^3 + H_4(\theta-\theta_0)^4\right] \\ & + \sum_\phi \left[V_1\left[1-\cos\left(\phi-\phi_1^0\right)\right] + V_2\left[1-\cos\left(2\phi-\phi_2^0\right)\right]\right. \\ & \left. + V_3\left[1-\cos\left(3\phi-\phi_3^0\right)\right]\right] + \sum_x K_x\chi^2 + E_{\text{UB}} \end{aligned} \tag{5}$$

$$\begin{aligned} E_{\text{cross-term}} = {} & \sum_b \sum_{b'} F_{bb'}(b-b_0)\left(b'-b_0'\right) \\ & + \sum_\theta \sum_{\theta'} F_{\theta\theta'}(\theta-\theta_0)\left(\theta'-\theta_0'\right) \\ & + \sum_b \sum_\theta F_{b\theta}(b-b_0)(\theta-\theta_0) \\ & + \sum_b \sum_\theta F_{b\theta}(b-b_0)\times[V_1\cos\phi + V_2\cos 2\phi \\ & + V_3\cos 3\phi] + \sum_{b'} \sum_\theta F_{b'\theta}\left(b'-b_0'\right)\left(b'-b_0'\right) \\ & \times[F_1\cos\phi + F_2\cos 2\phi + F_3\cos 3\phi] + \sum_\theta \\ & \times \sum_\phi F_{\theta\phi}(\theta-\theta_0)\times[V_1\cos\phi + V_2\cos 2\phi \\ & + V_3\cos 3\phi] + \sum_\phi \sum_\theta \sum_{\theta'} K_{\phi\theta\theta'}\cos\phi \\ & \times(\theta-\theta_0)\times\left(\theta'-\theta_0'\right) \end{aligned} \tag{6}$$

$$E_{\text{non-bond}} = \sum_{i>j}\left[\frac{A_{ij}}{r_{ij}^9} - \frac{B_{ij}}{r_{ij}^6}\right] + \sum_{i>j}\frac{q_i q_j}{\varepsilon r_{ij}} + E_{\text{H-bond}} \tag{7}$$

where q is the atomic charge, ε is the dielectric constant, and r_{ij} is the i–j atomic separation distance. b and b' are the lengths of two adjacent bonds, θ is the two-bond angle, ϕ is the dihedral torsion angle, and χ is the out-of-plane angle. b_0, $k_i(i=2-4)$, θ_0, $H_i(i=2-4)$, $\phi_i^0(i=1-3)$, $V_i(i=1-3)$, $F_{bb'}$, b_0', $F_{\theta\theta'}$, θ_0', $F_{b\theta}$, $F_{b\phi}$, $F_{b'\theta}$, $F_i(i=1-3)$, $F_{\theta\phi}$, $K_{\phi\theta\theta'}$, A_{ij}, and B_{ij} are fitted from quantum mechanics calculations and are implemented into the Discover module of Materials Studio [38], a powerful commercial atomic simulation program used in this paper.

2.3. Molecular model

Poly(methyl methacrylate) (PMMA) and polyethylene (PE) are well-known polymers used in a variety of engineering areas. Therefore, PMMA and PE, with 10 repeating units in each chain, are chosen as matrices in the study, which are also due to their simplicity and generic representation feature for polymer materials. The molecular model of PMMA and PE are shown in Fig. 1. (10, 10) SWNTs, which have diameters of 13.56 Å and lengths of 59.03 Å, are selected for the

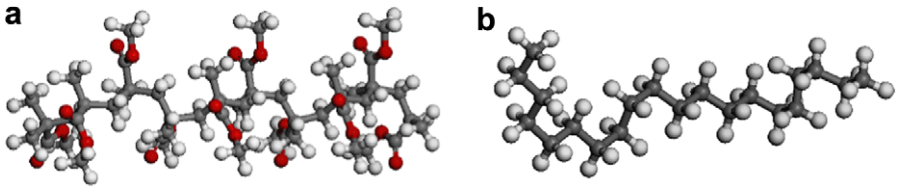

Fig. 1. Molecular model of PMMA and PE.

simulations of the SWNT–PMMA composites except special conditions. The unsaturated boundary effect was avoided by adding hydrogen atoms at the ends of the SWNTs. Each C–C bond length was 1.42 Å and C–H bond length was 1.14 Å. The hydrogen atoms had charges of +0.1268 e and the carbon atoms connecting hydrogen atoms had charges of −0.1268 e, thus the neutrally charged SWNTs were constructed.

The literature supplies numerous examples of addition reactions on nanotube surfaces [39]. Ying et al. [40] reported the grafting of aromatic rings on the side walls of SWNTs. In the present work, we used phenyl groups to functionalize the nanotube surface due to its simplicity and generic representation for the functionalization of CNTs. As we know, the dispersion degree of the SWNTs in the PMMA matrix can affect the interfacial bonding characteristics between the SWNTs and the PMMA matrix. However, if we consider the dispersion degree of the SWNTs, the computational system would be so large that it would cost too long a time for the simulation. Also, since the main goal of our research is to investigate the interfacial bonding characteristics between the SWNTs and the PMMA matrix, the SWNTs were assumed to be well dispersed in the PMMA matrix and the simulation results would be useful for the production of SWNTs-reinforced polymer composites as well. The composites, reinforced by pristine SWNT and the SWNTs on which 0.5%, 2.5%, 5%, 7.5%, or 10% of the carbon atoms had a bonded phenyl group, were simulated using MM and MD simulations. The chemical functionalization of the SWNTs has been performed by attaching functional groups to the surface of the CNTs through chemical covalent bonding and the functional groups were randomly end-grafted to the surface of the SWNTs. Fig. 2 shows the nanotube on which 2.5% of the atoms were attached by phenyl groups (the left panel) and the associated change in geometry of the atoms to which the phenyl groups are bonded (the right panel). The bonded nanotube atoms are "raised" away from the nanotube axes and the value of the strong covalent binding energy is 3.03 eV [41].

3. Results and discussion

The bonding strength between the SWNTs and the polymers can be evaluated by interfacial energy in the composites. Generally, the interaction energy is estimated from the difference between the potential energy of the composites system and the potential energy for the polymer molecules and the corresponding SWNTs as follows:

$$\Delta E = E_{\text{total}} - \left(E_{\text{SWNT}} + E_{\text{polymer}}\right) \tag{8}$$

where E_{total} is the total potential energy of the composite, E_{SWNT} is the energy of the nanotube without the polymer, and E_{polymer} is the energy of the polymer without the nanotube. In the other words, the interaction energy can be calculated as the difference between the minimum energy and the energy at an infinite separation of the nanotube and the polymer matrix [23,24,31]. The total interaction energy, ΔE, is twice the interfacial bonding energy γ scaled by the contact area A [25].

$$\gamma = \frac{\Delta E}{2A} \tag{9}$$

The magnitude of interfacial shear stress from the polymer matrix to the nanotubes is known to strongly influence the mechanical properties of nanotube composites. The pullout simulations were performed to characterize the interfacial shear stress of the composites. The pullout energy, E_{pullout}, is defined as the energy difference between the fully embedded nanotube and the complete pullout configuration [26]. The pullout energy is divided into three terms as follows [23]:

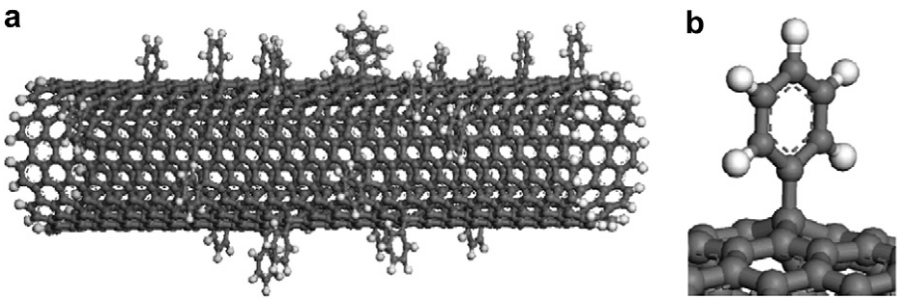

Fig. 2. Illustration of a (10, 10) SWNT with phenyl groups randomly chemisorbed to 2.5% of the carbon atoms.

$$E_{\text{pullout}} = E_2 - E_1 = \left(\Delta E_2 + E_{\text{SWNT2}} + E_{\text{polymer2}}\right) - \left(\Delta E_1 + E_{\text{SWNT1}} + E_{\text{polymer1}}\right) = \left(\Delta E_2 - \Delta E_1\right) + \left(E_{\text{SWNT2}} - E_{\text{SWNT1}}\right) + \left(E_{\text{polymer2}} - E_{\text{polymer1}}\right) \quad (10)$$

where E_2 and E_1 are the potential energy of the composite after and before the pullout simulation, respectively, E_{SWNT} and E_{polymer} are the potential energy of the nanotube and the polymer, respectively, and ΔE is the interaction energy between the nanotube and the polymer. The pullout energy can be related to the interfacial shear stress, τ_i, by the following relation:

$$E_{\text{pullout}} = \int_{x=0}^{x=L} 2\pi r(L-x)\tau_i \mathrm{d}x = \pi r \tau_i L^2 \quad (11)$$

$$\tau_i = \frac{E_{\text{pullout}}}{\pi r L^2} \quad (12)$$

where r and L are the outer radius and length of the SWNT, respectively, and x is the coordinate along the longitudinal tube axis [26].

In the simulations, each of the composite systems was composed of a fragment of SWNT totally embedded inside the amorphous polymer matrix. A model of the composite system embedded by the pristine SWNT, which consisted of a supercell in the range of 57 Å × 57 Å × 62 Å, is shown in Fig. 3. For SWNT–PMMA system, each of the configurations was initiated by randomly generating 112 PMMA molecular chains surrounding the SWNT using an initial density of 1.2 g/cm^3. For SWNT–PE system, each of the configurations was initiated by randomly generating 247 PE molecular chains surrounding the SWNT using an initial density of 0.9 g/cm^3. The models were put into an NPT ensemble simulation with a pressure of 10 atm and a temperature of 300 K for 10 ps at a time step of 1 fs while holding the nanotube rigid. The purpose of this step was to slowly compress the structure of the matrix polymers to generate initial amorphous matrix with the correct density and low residual stress. The matrix polymers were then put into an NVT ensemble simulation and equilibrated for 20 ps with a time step of 0.2 fs with rigid nanotubes. After that, the composite systems were further equilibrated for 40 ps at a time step of 2 fs with non-rigid nanotubes to create a zero initial stress state using NVT ensembles. The energy of the composite systems was minimized to achieve the strongest bonding between the nanotubes and the polymer as shown in Figs. 4 and 5 [23,31]. Finally, the interfacial bonding energy and interfacial shear stress were calculated through pullout simulations.

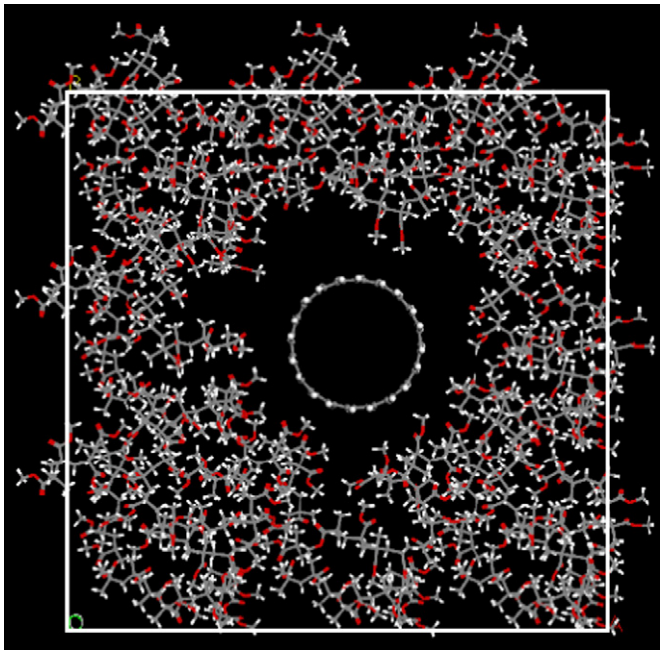

Fig. 3. Cross-section view of SWNT–PMMA system before simulation.

3.1. Interfacial bonding for pristine SWNT

The pullout simulations of the SWNT were performed in order to characterize the interfacial shear strength of the composites. The SWNT was pulled out of the polymer matrix along the nanotube axis direction. Fig. 6 shows the snapshots of the pullout simulations. The potential energy, interaction energy, and interfacial bonding energy were plotted against the displacement of the SWNT from the polymer matrix, as shown in Figs. 7 and 8. During the pullout, the interaction energy changed with the displacement linearly and decreased toward a value of zero, as shown in Figs. 7a and 8a. This is due to the stable interfacial binding interaction and the decrease of contact area during the pullout. Figs. 7b and 8b indicate that the pullout energy of the SWNT–polymer composite system was increased as the SWNT was pulled out of the polymer. The interfacial binding energy was kept constant with a value of 0.1 kcal/mol Å^2 during the pullout, as shown in Figs. 7c and 8c. After the SWNT was completely pulled out of the polymer, the potential energy of the system was leveled off and the interaction energy was then kept zero.

3.2. Influence of chemical functionalization

The SWNTs and the polymer matrix were not held fixed in the pullout simulation. Therefore, the pullout energy has been influenced by the deformation of the nanotubes and polymer during the pullout. Figs. 9 and 10 show the interaction energy changed with the displacement nearly linearly during the pullout, which is due to the stable interfacial binding interaction between the SWNTs and the polymer. However, the interaction energy would keep zero after the nanotubes were completely pulled out of the polymer because there was no interaction between the nanotubes and the polymer [27].

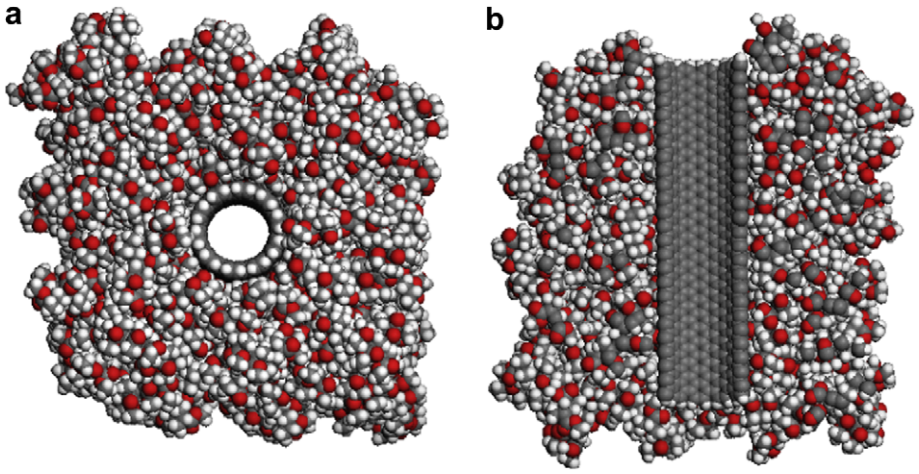

Fig. 4. Molecular model of SWNT–PMMA composite system: (a) top view; (b) section view.

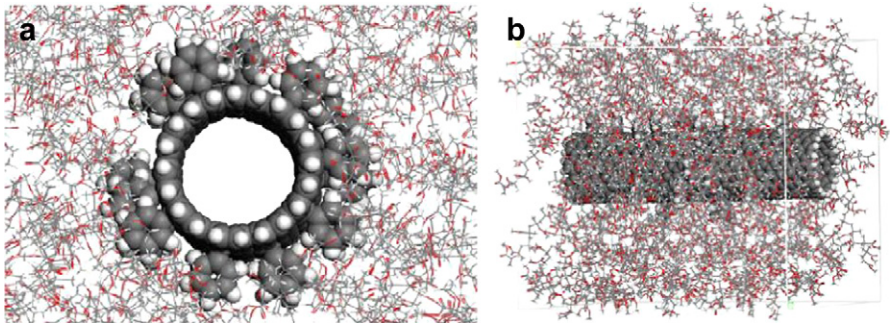

Fig. 5. Illustration of the composite embedded by a (10, 10) SWNT with phenyl groups randomly chemisorbed to 2.5% of the carbon atoms: (a) top view; (b) side view.

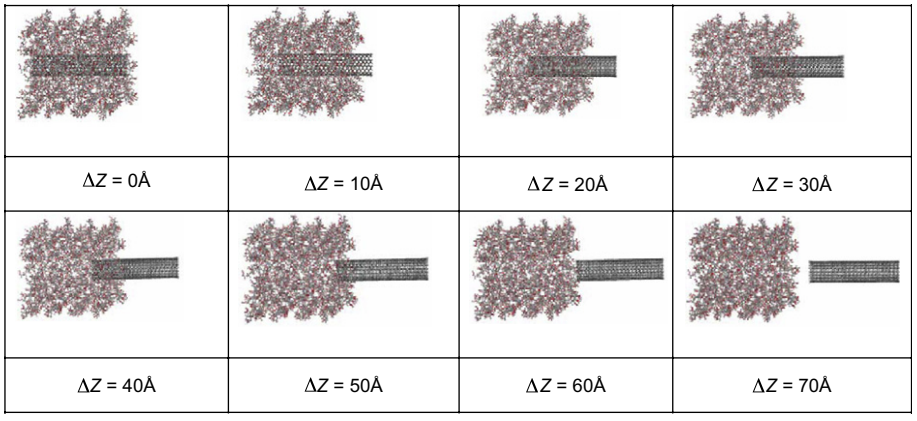

Fig. 6. Snapshots from the MD simulation of the pullout of the SWNT.

Plotted in Figs. 11a,b and 12a,b are the calculated interaction energy and interfacial bonding energy for SWNTs as a function of the degree of functionalization. When the degree of functionalization is increased, the interaction energy and interfacial bonding energy between the simulated SWNTs and the polymer monotonically increase toward a magnitude value, which is about four times the value for pristine SWNT. The interfacial bonding, which appears to be critically dependent on the nanotube–polymer interface surface area, will increase linearly with the total interface surface area [10]. When the SWNT is chemically attached with phenyl groups, the contact area between the nanotube and the polymer matrix will be drastically increased, which will cause the increase of the interfacial bonding between the nanotube and the polymer.

Figs. 11c and 12c show the growth and saturation with higher degrees of functionalization. The results show that the shear stress of nanotube–polymer interface with weak nonbonded interactions can be increased by about 1000% with

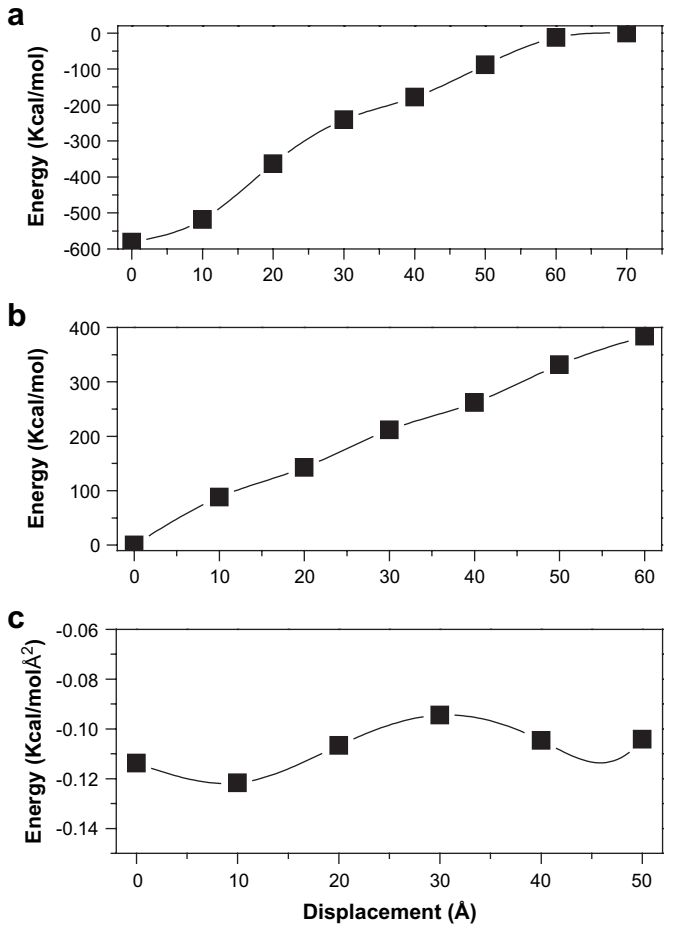

Fig. 7. Energy plots during the pullout of the SWNT from the PMMA matrix; (a) interaction energy; (b) pullout energy; (c) interfacial bonding energy.

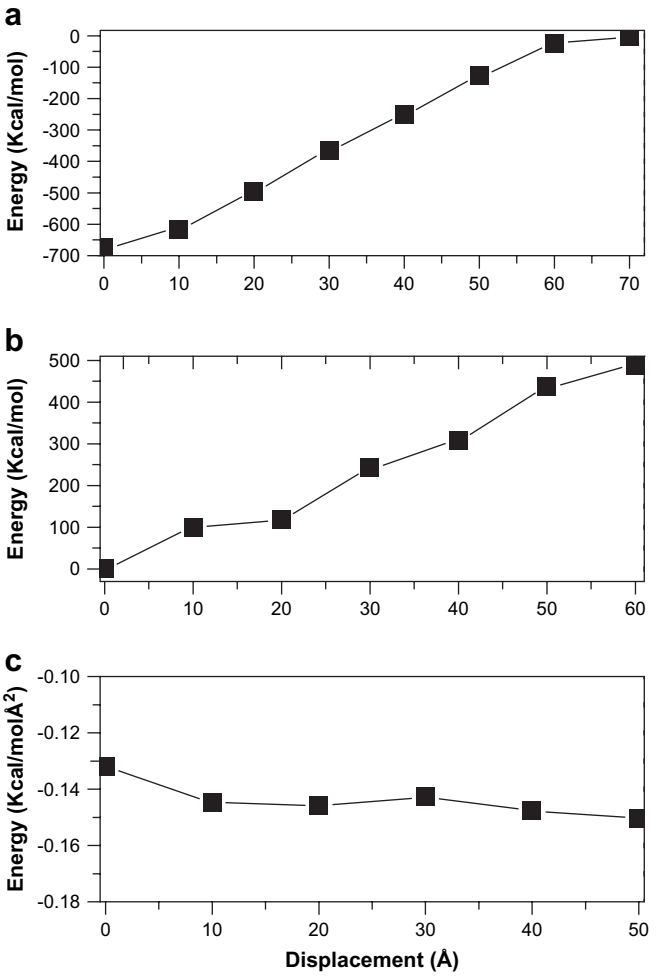

Fig. 8. Energy plots during the pullout of the SWNT from the PE matrix; (a) interaction energy; (b) pullout energy; (c) interfacial bonding energy.

the introduction of a relatively low density ($\leq$5%) of chemical attachment. However, the shear stress increases only weakly with the introduction of a relatively high density (>5%) of chemical attachment. When the functional groups of SWNT were successfully embedded into the polymer matrix, which may possibly link SWNTs with the polymer matrix, the shear stress could be effectively increased. The successful embedding could happen at a low density of functionalization and thus an effective enhancement of the shear stress could be attained. However, when the density of functionalization becomes higher, some functional groups may only contact with the other functional groups, which may lead to a direct result that the effective contact surface area between the functional groups and the polymer matrix couldn't be strongly increased any more, and thus there is only a weak increase of the shear stress.

Although the covalent attachment of functional groups to the surface of nanotubes can improve the efficiency of load transfer, these functional groups might introduce defects on the walls of the perfect structure of the nanotubes, which will lower the strength of the nanotube filler. Some models predict that the change in mechanical properties of the SWNTs with lower level ($\leq$10%) of functionalization is negligible [27]. So SWNT with 5% level of functionalization may be the feasible nanotube type for reinforcement, which could improve the efficiency of load transfer with negligible influence on the mechanical properties of the SWNT. It also supports

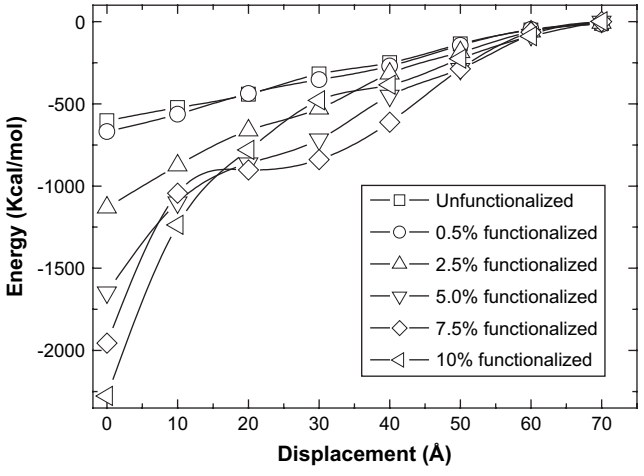

Fig. 9. Interaction energy plots during the pullout of the SWNT from the PMMA matrix.

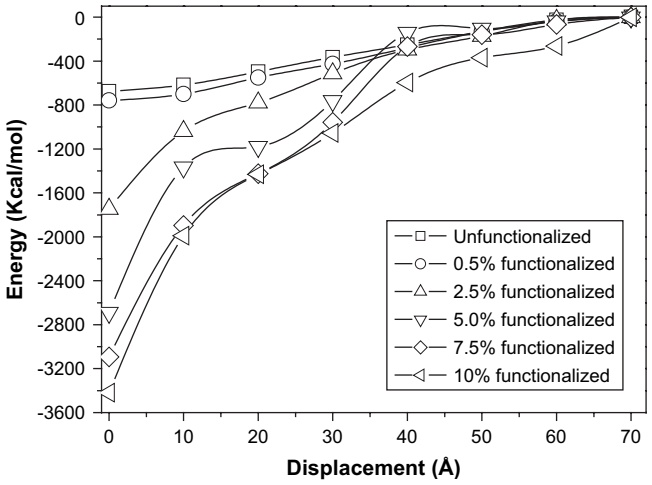

Fig. 10. Interaction energy plots during the pullout of the SWNT from the PE matrix.

suggestions that chemical attachment of nanotubes during processing may be in part responsible for the enhanced stress transfer observed in some systems of the nanotube–polymer composites.

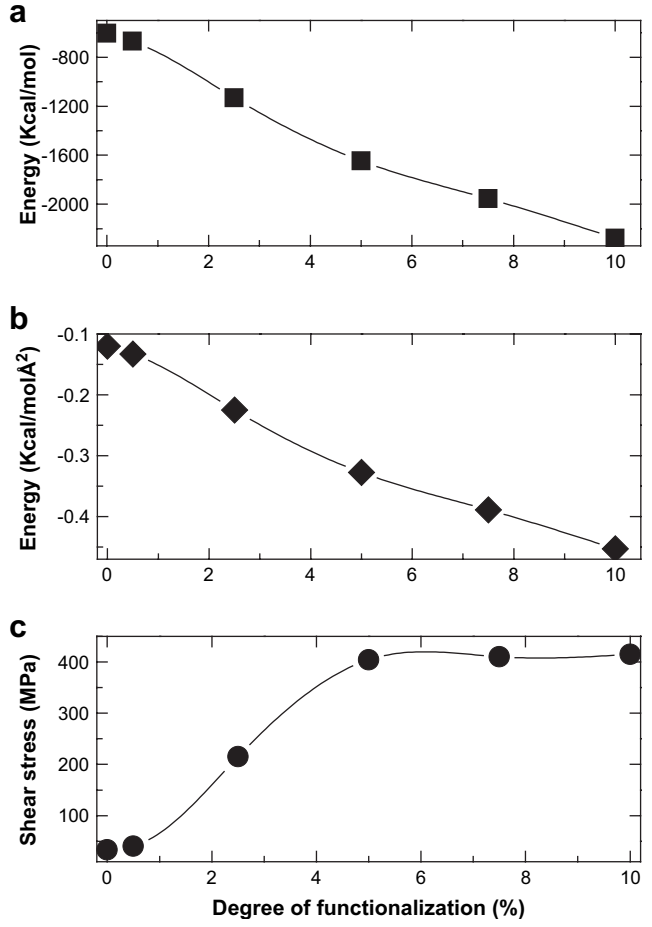

Fig. 11. Influence of chemical functionalization on the interfacial bonding characteristics of SWNT for SWNT–PMMA system; (a) interaction energy; (b) interfacial bonding energy; (c) shear stress.

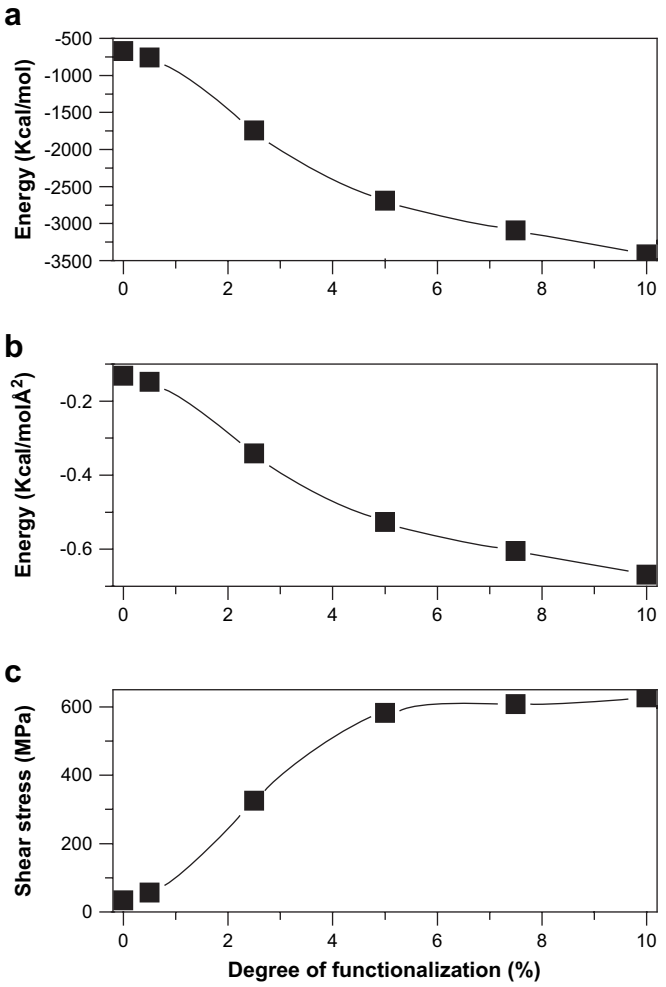

Fig. 12. Influence of chemical functionalization on the interfacial bonding characteristics of SWNT for SWNT–PE system; (a) interaction energy; (b) interfacial bonding energy; (c) shear stress.

4. Conclusions

In summary, we have used MM and MD simulations to study the effect of chemical functionalization on the interfacial bonding characteristics between the SWNTs and the polymer matrix. The simulations show that functionalization of nanotubes at low densities of functionalized carbon atoms drastically increase their interfacial bonding and shear stress between the nanotubes and the polymer matrix. This indicates that increasing the load transfer between SWNTs and a polymer matrix in a composite via chemisorption may be an effective way and chemical attachment of nanotubes during processing may be in part responsible for the enhanced stress transfer observed in some systems of the nanotube–polymer composites. Furthermore, this suggests the possibility to use functionalized nanotubes to effectively reinforce other kinds of polymer-based materials as well.

Acknowledgments

This work was supported by CNPC Innovation Fund under Contract No. 06E1024, the Key Project of Chinese Ministry of

Education under Contract No. 106036, and Shandong Natural Science Foundation under Contract No. Y2005A10.

References

[1] Iijima S. Nature 1991;354:56–8.
[2] Cheng Y, Liu GR, Li ZR, Lu C. Physica A 2006;367:293–304.
[3] Zheng QB, Xue QZ, Yan KY, Hao LZ, Li Q, Gao XL. J Phys Chem C 2007;111(12):4628–35.
[4] Wagner HD, Lourie O, Feldman Y, Tenne R. Appl Phys Lett 1998; 72(2):188–90.
[5] Andrews R, Jacques D, Rao AM, Rantell T, Derbyshire F, Chen Y, et al. Appl Phys Lett 1999;75(9):1329–31.
[6] Ajayan PM, Schadler LS, Giannaris C, Rubio A. Adv Mater 2000; 12(10):750–3.
[7] Qian D, Dickey EC, Andrews R, Rantell T. Appl Phys Lett 2000; 76(20):2868–70.
[8] Cadek M, Coleman JN, Barron V, Hedicke K, Blau WJ. Appl Phys Lett 2002;81(27):5123–5.
[9] Dalton AB, Collins S, Munoz E, Razal JM, Ebron VH, Ferraris JP, et al. Nature 2003;423:703.
[10] Cadek M, Coleman JN, Ryan KP, Nicolosi V, Bister G, Fonseca A, et al. Nano Lett 2004;4(2):353–6.
[11] Yan KY, Xue QZ, Zheng QB, Hao LZ. Nanotechnology 2007; 18(25):255705.
[12] Kim B, Lee J, Yu I. J Appl Phys 2003;94(10):6724–8.
[13] Ramasubramaniam R, Chen J, Liu HY. Appl Phys Lett 2003; 83(14):2928–30.
[14] Sandler JKW, Kirk JE, Kinloch IA, Shaffer MSP, Windle AH. Polymer 2003;44:5893–9.
[15] Clancy TC, Gates TS. Polymer 2006;47:5990–6.
[16] Wei CY, Srivastava D, Cho K. Nano Lett 2002;2(6):647–50.
[17] Pham JQ, Mitchell CA, Bahr JL, Tour JM, Krishanamoorti R, Green PF. J Polym Sci B 2003;41(24):3339–45.
[18] Kymakis E, Amaratunga GAJ. Appl Phys Lett 2002;80(1):112–4.
[19] Shaffer MSP, Windle AH. Adv Mater 1999;11(11):937–41.
[20] Lozano K, Barrera EV. J Appl Polym Sci 2000;79(1):125–33.
[21] Sen R, Zhao B, Perea D, Iktis ME, Hu H, Love J, et al. Nano Lett 2004;4(3):459–64.
[22] Li XD, Gao HS, Scrivens WA, Fei DL, Xu XY, Sutton MA, et al. Nanotechnology 2004;15:1416–23.
[23] Gou J, Minaie B, Wang B, Liang ZY, Zhang C. Comput Mater Sci 2004; 31:225–36.
[24] Al-Haik M, Hussaini MY. J Appl Phys 2005;97:074306.
[25] Lordi V, Yao N. J Mater Res 2000;15(12):2770–9.
[26] Liao K, Li S. Appl Phys Lett 2001;79(25):4225–7.
[27] Frankland SJV, Caglar A, Brenner DW, Griebel M. J Phys Chem B 2002; 106(12):3046–8.
[28] Wong M, Paramsothy M, Xu XJ, Ren Y, Li S, Liao K. Polymer 2003; 44:7757–64.
[29] Yang MJ, Koutsos V, Zaiser M. J Phys Chem B 2005;109(20):10009–14.
[30] Wei CY. Appl Phys Lett 2006;88:093108.
[31] Gou J, Liang ZY, Zhang C, Wang B. Compos B 2005;36:524–33.
[32] Maple JR, Hwang MJ, Stockfisch TP, Dinur U, Waldman M, Ewig CS, et al. J Comput Chem 1994;15(2):162–82.
[33] Sun H. J Comput Chem 1994;15(7):752–68.
[34] Sun H. J Phys Chem B 1998;102(38):7338–64.
[35] Sun H, Ren P, Fried JR. Comput Theor Polym Sci 1998;8(1/2):229–46.
[36] Rigby D, Sun H, Eichinger BE. Polym Int 1998;44(3):311–30.
[37] Grujicic M, Cao G, Roy WN. Appl Surf Sci 2004;227:349–63.
[38] <http://www.accelrys.com/products/mstudio/modeling/polymersandsimulations/discover.html>.
[39] Banerjee S, Hemraj-Benny T, Wong SS. Adv Mater 2005;17(1):17–29.
[40] Ying YM, Saini RK, Liang F, Sadana AK, Billups WE. Org Lett 2003; 5(9):1471–3.
[41] Padgett CW, Brenner DW. Nano Lett 2004;4(6):1051–3.